

## Microstructure and Microhardness Study of Aluminium Graphene Composite Made by Laser Additive Manufacturing

A. Mandal<sup>a#</sup>, J. K. Tiwari<sup>a#</sup>, N Sathish<sup>a\*</sup>, C. P. Paul<sup>b,c</sup>, S. K. Mishra<sup>b</sup>, Venket Ch A N<sup>a</sup>, A K Singh<sup>a</sup>, S A R Hashmi<sup>a</sup>

<sup>a</sup> CSIR-Advanced Materials and Processes Research Institute, Bhopal, India.

<sup>b</sup> Laser Additive Manufacturing Lab, Raja Ramanna Centre for Advanced Technology, Indore, India.

<sup>c</sup> Homi Bhabha National Institute, BARC Training School Complex, Anushakti Nagar, Mumbai, India

<sup>A</sup>Dr. N. Sathish, Senior Scientist, Advanced Materials and Processes Research Institute, Bhopal, India.

*Received 18 September 2018; revised 21 January 2019; accepted 22 January 2019*

Laser additive manufacturing (LAM) is one of the advanced manufacturing technologies capable of manufacturing complex engineering components with superior material properties by layer by layer deposition of material directly from CAD model. Layer-by-layer addition of material empowers LAM in selective deposition of pre-defined composition of material shaping the engineering components making it a feature based design and manufacturing technology. The LAM built components largely depends on LAM processing parameters and the quality of single deposited layer. Hence selection of appropriate processing parameters is one of the mandatory requirements for achieving superior mechanical properties LAM built components. This paper reports the LAM of aluminium/grapheme (Al-G) composite on Al and SS substrate. 2 kW fibre laser based additive manufacturing with 2 mm laser beam diameter at substrate was used to deposit Al-G layers (Al + 1%wt G) at different combinations of laser scanning speed and laser power. Effect of laser power and scanning speed on the quality of deposited layers was investigated and optimum parametric window was identified. The Optimum range of energy intensity is 50 to 400 J/mm which favours material deposition ( $< 50P/v - < 400 J/mm$ ). Thus prepared samples were subjected to optical microscopy, scanning electron microscopy and microhardness measurements. A good quality continuous track is observed at 108 J/mm energy intensity and there is very slight change in hardness observed on Al substrate). A significant increase in micro hardness is observed on SS substrate. The maximum value of HV is 463.6 at 0.6 m/min. laser scanning speed and 1.2 kW laser power. These LAM built Aluminium grapheme composite have potential applications in the field of light weight and high strength material for manufacturing of complex shape and cellular structure.

**Keywords:** Graphene, Graphene composites, Aluminium, Metal Matrix composites, Additive manufacturing, Microstructure and Micro Hardness, Laser Additive Manufacturing.

Laser Additive Manufacturing (LAM) is one of the fastest growing techniques for fabrication of complex parts which finally expands the boundaries of possibilities in engineering applications. In general, LAM uses metal powder, which is melted and deposited layer by layer on the substrate to create any object designed in CAD software. Since the process melts the powder completely could achieve nearly 100% density and mechanical properties superior to that of bulk cast component. In industries, LAM is being introduced for production of small and complex components and fabrication of functionally graded material having variation in properties as move across the layer<sup>1,2</sup>.

Process parameters of LAM (like laser power, laser scanning speed, spot dia., laser wavelength etc.) have to be controlled very precisely for achieving desired

properties in the final component<sup>3-6</sup>. However, the correlations between these parameters are not very much clear yet. Elaborative experimentation is required to understand the influence of these parameters on each other and also on the quality of final component<sup>7</sup>.

### **Problem associated with Additive Manufacturing**

In most of the additive manufacturing techniques the energy delivered by laser, melts the metal powder and creates molten metal pool, which has a tendency to shrink during solidification and sometimes this molten metal takes the shape of spherical balls during solidification to reduce its surface energy this phenomenon is known as balling effect<sup>8, 9, 3</sup>. Balling should be avoided as it degrades the quality of finished component. Balling results in increasing surface roughness, which directly influence on the topography and dimensional accuracy, it also

\*Corresponding author (E-mail: nsathish@ampri.res.in)

introduces porosity which deteriorates mechanical properties of component<sup>10</sup>. Balling effect in the first deposited layer (adjacent to substrate) is also occurs due to inappropriate wetting between molten metal and substrate. The schematic diagram of wetting phenomenon on substrate is shown in Fig. 1.

There are many published reports on optimization of process parameters and methods use to avoid balling for different materials. Childs *et al.*<sup>11</sup> have studied the balling effect for SS314 and tool steel H13 under different laser powers and scanning speeds and optimize these parameters which are useful in choosing proper parameters for preventing balling. I. Yadroitsev *et al.*<sup>4</sup> analyzed the variation of energy intensity (P/v ratio) on the quality of scan track. Dadbakhsh *et al.*<sup>12</sup> explained the effects of process parameters on the properties of Al/Fe<sub>2</sub>O<sub>3</sub> composite fabricated by LAM. TiC/Ti functionally graded composite are fabricated by W. Liu *et al.*<sup>13</sup> using laser engineered net shaping (LENS) system and studied the microhardness from one end to other. Majority of work on additive manufacturing are on Al or its alloy very few work is reported on its composite. To the best of our knowledge very few works are reported on Al/graphene nanocomposite with assist of LAM. In the present work, we report the study of quality of the single track of Al/1 wt. % graphene composites under different combination of scan speed and laser power. Cross-section of deposited tracks was examined under FESEM, optical microscopy and microhardness test.

#### Experimental procedure

Al powder with particle size 15  $\mu\text{m}$  and 1 wt. % graphene powder (2-10 nm thickness and 10-15  $\mu\text{m}$  particle size) are mixed thoroughly in tumbler for 20 minute. 2 kW fibre laser based LAM powder feed system with a wavelength of 1.08  $\mu\text{m}$  having spot size of 2 mm at substrate was used in the current study<sup>14</sup>. The experiment was performed in argon inert atmosphere to avoid oxidation during melting. LAM process parameters are categorized into four groups as shown in Fig. 2.

The present study focus on mainly three parameters i.e. laser power, laser scanning speed and substrate material (Aluminium and SS). Total four samples were prepared; two samples by keeping constant laser power and other two samples are by keeping constant laser scanning speed. For Al substrate, sample no. 1 is made by keeping constant laser power at 1.8 kW and five tracks are deposited at different scanning speed 0.1, 0.3, 0.5, 0.7, 1.0 m/min and sample no. 2 is made

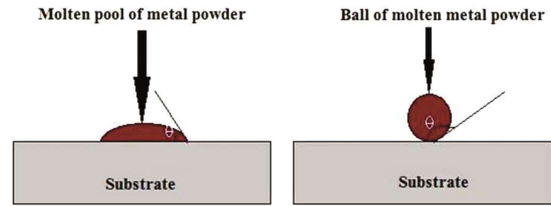


Fig. 1 – Wetting phenomenon between molten metal powder and substrate.

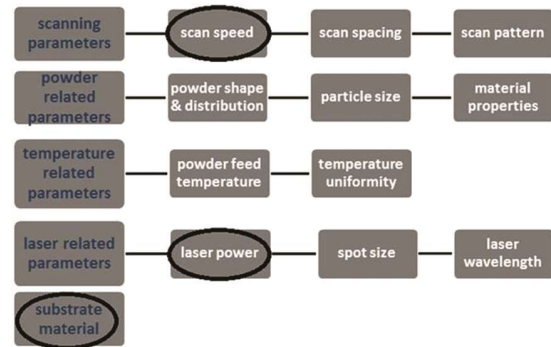


Fig. 2 – LAM important parameters.

by keeping constant laser scanning speed 1.2m/min and varying laser power of 1.8, 1.6, 1.4, 1.2, 1.0 kW. Similarly for SS substrate, sample no. 3 is made by keeping scanning speed constant at 1.2 m/min and varying laser power 1, 1.2, 1.4, 1.6, 1.8 kW. Sample no. 4 is made by keeping constant laser power at 1.2 kW by varying scanning speed of 1.2, 1.1, 1.0, 0.9, 0.8, 0.7, 0.6 m/min. Description of tracks are given in Table 1.

The microstructure of cross-section of deposited layers is studied by FESEM micrograph at various magnifications. Vickers microhardness test is performed on polished and etched cross-section surface using LAICA microhardness tester (Model: Vm 50). For sample 1 and 2 test load was kept at 100 gf and for sample 3 & 4 test load was kept at 200 gf.

#### Results and discussion:

Microstructure and hardness studies are carried out for all tracks to identify the combined effect of laser scan speed and laser power on track formation. The results are analysed in the light of energy intensity and wetting characteristic of molten powder on substrate. Temperature of the metal powder increases significantly due to the absorption of laser power leads to the formation of molten pool. As scan speed of laser increases, the liquid metal gets spatter and takes spherical shape. These droplets are deposited on the periphery of the track as well as on the sides of the

Table 1 – Description of samples.

	Al Substrate				SS Substrate			
	Sample no. 1		Sample no. 2		Sample no. 3		Sample no. 4	
	Power (KW)	Scanning speed (m/min)						
Track 1	1.8	0.1	1.8	1.2	1	1.2	1.2	1.2
Track 2	1.8	0.3	1.6	1.2	1.2	1.2	1.2	1.1
Track 3	1.8	0.5	1.4	1.2	1.4	1.2	1.2	1.0
Track 4	1.8	0.7	1.2	1.2	1.6	1.2	1.2	0.9
Track 5	1.8	1.0	1.0	1.2	1.8	1.2	1.2	0.8
Track 6	--	--	--	--	--	--	1.2	0.7
Track 7	--	--	--	--	--	--	1.2	0.6

track. This phenomenon is known as balling effect and it degrades the properties of the final component<sup>8</sup>. When wettability of the molten metal and substrate is good, the balling effect reduces significantly in the layer adjacent to substrate. With poor wettability the width of the track narrows and contact area with substrate reduces which finally may lead to the misalignment of whole structure.

### Effect of Scan Speed Variation

#### Microstructure and topographic study

In this experiment for sample no. 1 and 4, laser scanning speed is varying and power is kept constant. Fig. 3 depicts the optical image of cross-section of the tracks deposited on sample no. 4.

The microstructure of cross-section of deposited layers is studied by FESEM micrograph at various magnifications. Vickers microhardness test is performed on polished and etched cross-section surface using LAICA microhardness tester (Model: Vm 50). For sample 1 and 2 test load was kept at 100 gf and for sample 3 & 4 test load was kept at 200gf.

The depth of the molten pool on SS substrate decreases slightly as scan speed increases from 0.6 to 1.2 m/min at constant power 1.2 kW and track width also reduces continuously on increasing scan speed due to reduction in energy intensity (Fig. 4a). During fabrication of any component through LAM the selection of appropriate range of energy intensity is very necessary to obtain good quality tracks and minimize the defects in tracks.

The depth of the molten pool on SS substrate decreases slightly as scan speed increases from 0.6 to 1.2 m/min at constant power 1.2 kW and track width also reduces continuously on increasing scan speed due to reduction in energy intensity (Fig. 4a). During fabrication of any component through LAM the

selection of appropriate range of energy intensity is very necessary to obtain good quality tracks and minimize the defects in tracks.

In sample no. 1 energy intensity reduces with increase in scan speed (Table 2). Initially scan speed of laser is very low for track 1 of sample no. 1 which is not sufficient for material deposition and further increase in scan speed leads to increase in track width as shown in Fig. 4b. Very low energy intensity is not favourable it may results in insufficient melting of metal powder that subsequently causes porosity<sup>15</sup> as seen in Fig. 5a.

Noriko Read *et al.*<sup>16</sup> investigated the effect of scanning speed and laser power on porosity. Splashing of molten metal can also cause porosity<sup>17</sup>. At 0.1 m/min. scan speed energy intensity is 1125 J/mm results high peak temperature of the molten pool due to which the deposited material flashes off and creates only heat affected zone on the substrate as shown in Fig. 5e.

#### Microhardness study

Microhardness of sample no. 1 initially decreases and starts to increase as scan speed increases. Highest microhardness obtained at 0.1 m/min i.e. 79 HV which is very close to substrate microhardness 88.16 HV. Material is not deposited at 0.1m/min scan speed and fusion zone is created by laser heating, which results microhardness at 0.1m/min scan speed is closes to substrate. The microhardness at 0.5 m/min is minimum at 68 HV which may be due to increasing porosity at higher scanning speed. Variation of microhardness is shown in Fig. 6 a.

A similar trend in microhadness variation is obtained in case of sample no. 4 i.e. on SS substrate. The decrement in microhardness with increase in scan speed is may be due to the increased porosity and

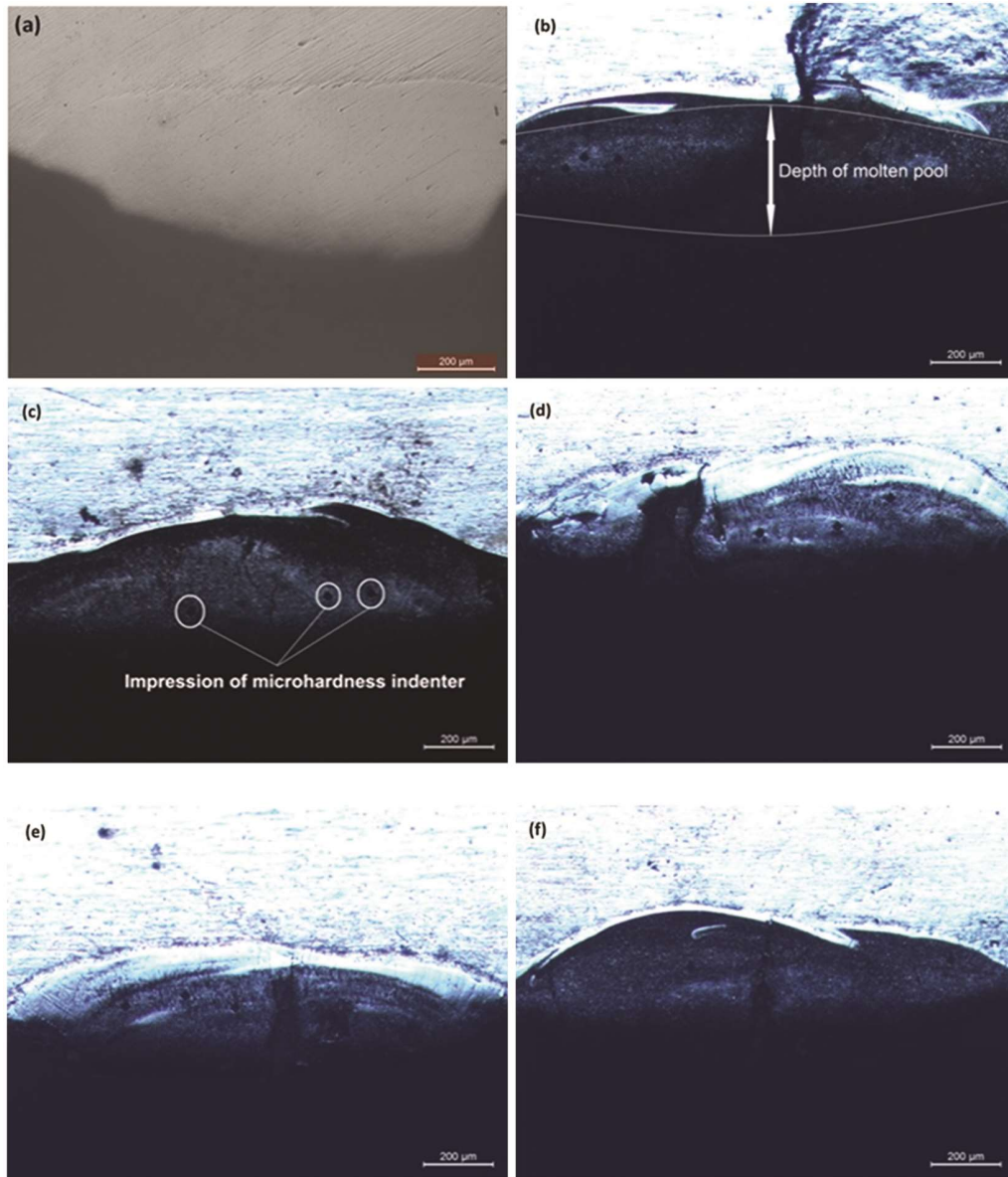


Fig. 3 – Interface images of different tracks of Al + 1 % graphene sample deposited on SS substrate at constant power= 1.2KW and varying scan speed (a) 0.6 m/min., (b) 0.7 m/min., (c) 0.8 m/min., (d) 0.9 m/min., (e) 1.0m/min., (f) 1.1m/min.

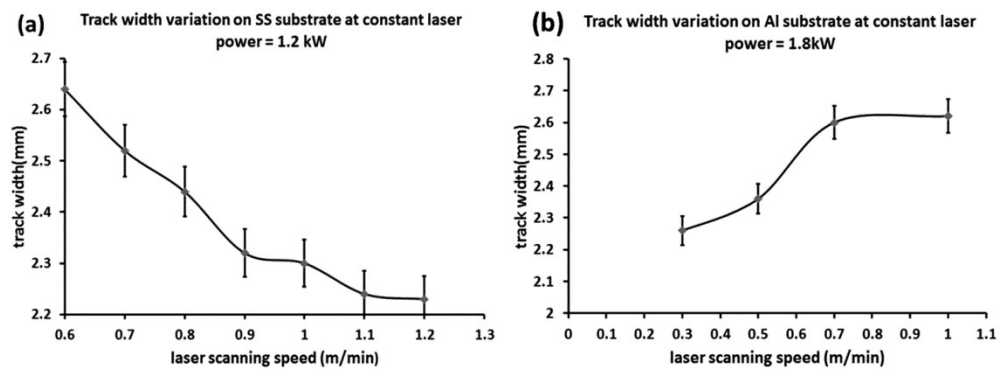


Fig. 4 – Track width variations with varying laser scanning speed (a) SS substrate (sample no. 4), (b) Al substrate (sample no. 1)

splashing molten pool<sup>18</sup>. Minimum hardness is 361.6 HV at 1.0 m/min scanning speed and further increase in scan speed resulting significant increase in microhardness (Fig. 6b).

**Effect of Laser Power variation**

**Microstructure and topographic study**

In present study for sample no. 2 and sample no. 3, laser power is varying and scanning speed is kept constant. In sample no. 2 laser power is varied from 1.0 to 1.8 kW and scan speed is kept constant at

Table 2 – Energy intensity per unit length for different tracks.

	Energy per unit length (P/V) in J/mm			
	Sample no. 1	Sample no. 2	Sample no. 3	Sample no. 4
Track 1	1125	90	50	60
Track 2	400	80	60	66
Track 3	216	70	70	72
Track 4	154	60	80	80
Track 5	108	50	90	90
Track 6	--	--	--	103
Track 7	--	--	--	120

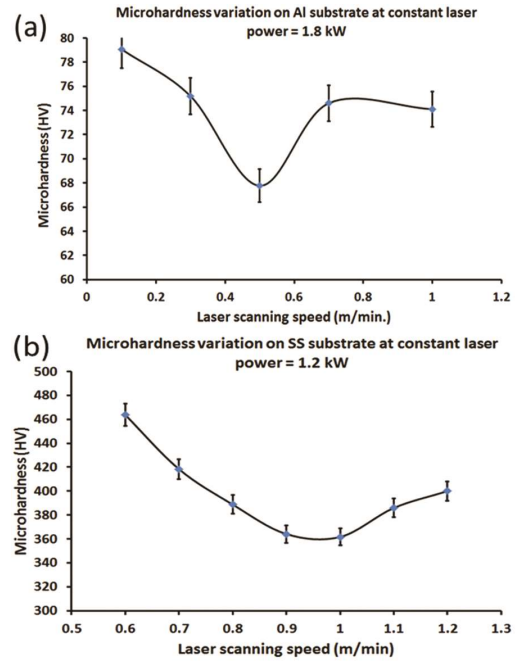


Fig. 6 – Variation in microhardness with varying scanning speed (a) Al substrate (sample no. 1), (b) SS substrate (sample no. 4).

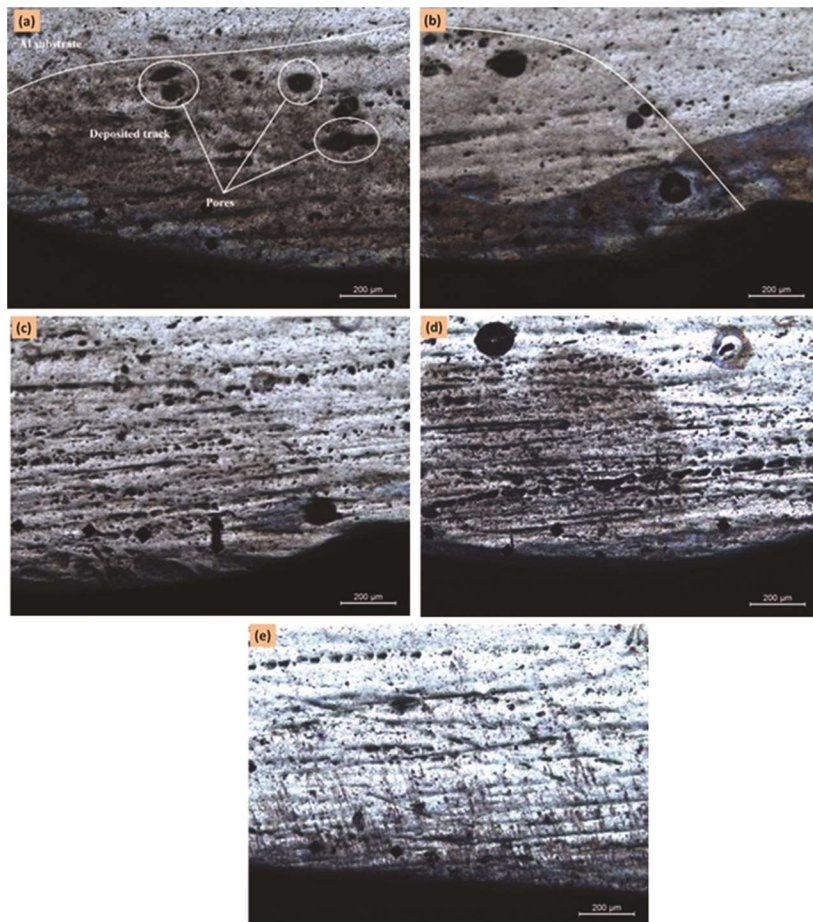


Fig. 5 – Microscopic images of cross section of sample no. 1 (a) 1.0 m/min (b) 0.7 m/min (c) 0.5 m/min (d) 0.3 m/min (e) 0.1 m/min.

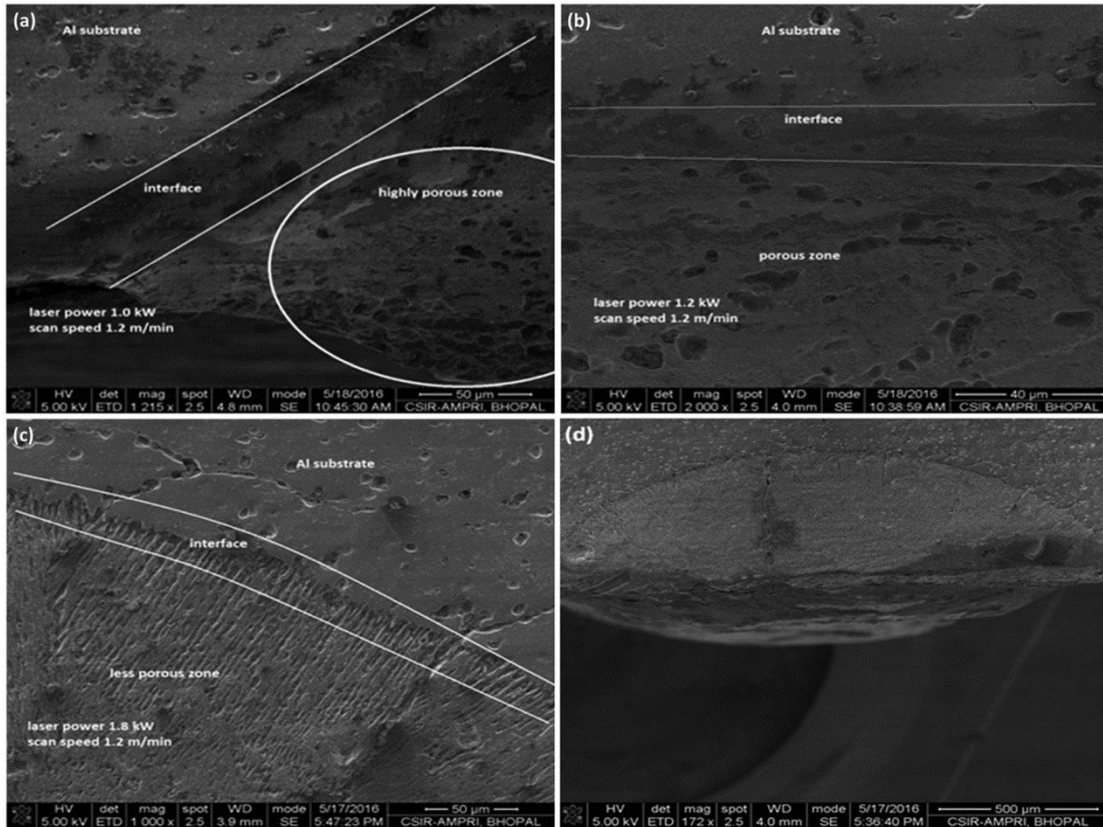


Fig. 7 – FESEM images of sample no. 2

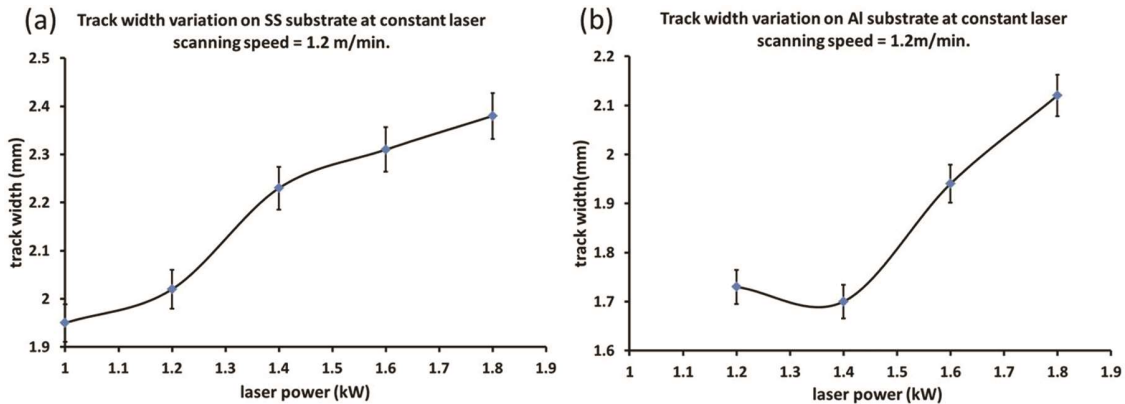


Fig. 8 – Track width variations with varying laser powers (a) SS substrate (sample no. 3), (b) Al substrate (sample no. 2)

1.2 m/min. Input energy intensity increases with increase in laser power. Figure 7 depicts the porosity variation with increasing laser power. The region below the interface is porous and porosity of this region mainly depends on the energy intensity. It is observed by the FESEM images that porosity reduces slightly by increasing laser power eventually due to increase in energy intensity. Similar phenomenon is also observed in track 5 of sample no. 1 as already discuss above. So in order to achieve highly dense (less porous) tracks, high

laser power is required<sup>19</sup> which is sufficient to melt the metal powder properly. It is also believed that due to the high reflectivity of Al (91%), lesser amount of energy is absorbed and majority of energy gets reflected<sup>20</sup>. Simultaneously higher heat dissipation occurs due to high thermal conductivity of Al (146 Wm-1K-1)<sup>21</sup>. Hence, width of tracks on Al substrate is lower than tracks width deposited on SS substrate for same parameters as shown in graph (Fig. 8). Track width is measured from cross-section as described in Fig. 9.

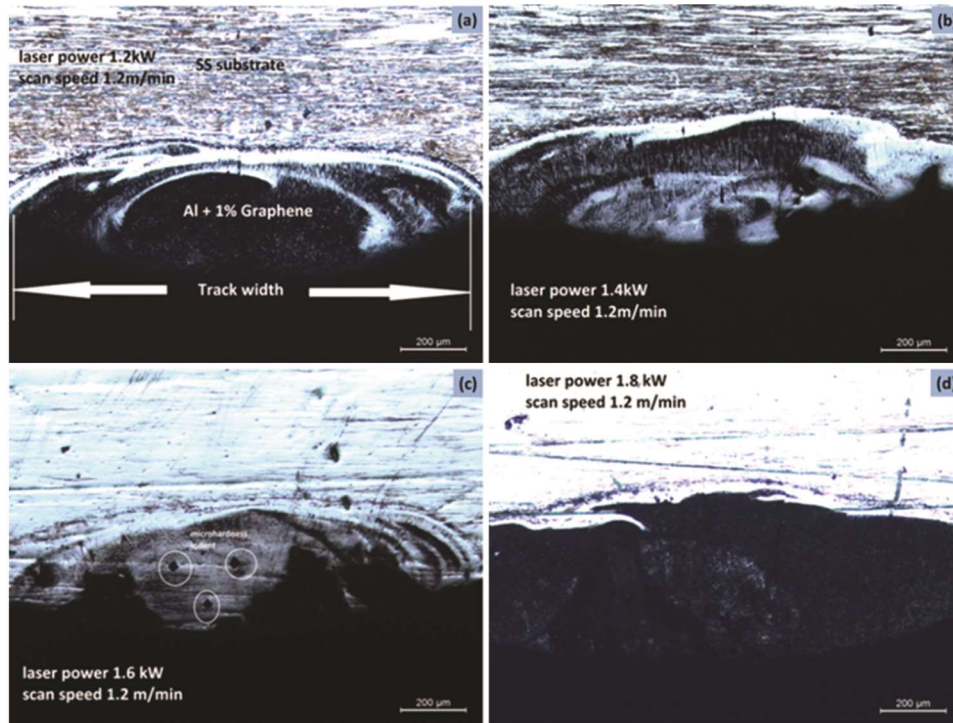


Fig. 9 – Increase width of track with increasing power (Sample no. 3).

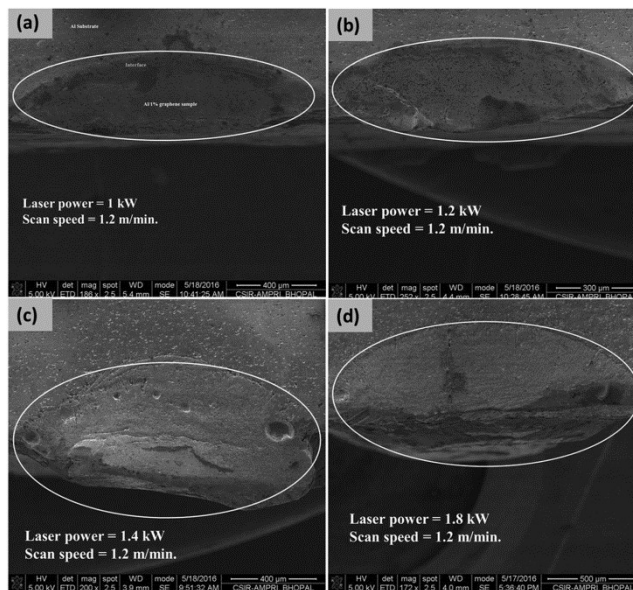


Fig. 10 – Sharpening of curvature along with increasing power causes increased remelted zone depth on Al substrate (sample no. 2).

### Microhardness study

Microhardness variation of sample 2 is shown in Fig. 11a which increases with increase in laser power and maximum value of 76.8 HV observed at 1.6 kW. It further decreases on increasing laser power. The microhardness of the Al substrate is 92 HV, which is higher than the microhardness of deposited track due to the porosity along with the microstructure of the

deposited layer. At low laser power (1 kW) P/v ratio is 50 J/mm which is insufficient to melt the powder on Al substrate so, track is not deposited and heat affected zone is negligible<sup>22</sup>.

The microhardness of SS substrate for sample 3 is 214.4 HV which is significantly lesser than the microhardness of deposited tracks. Figure 12b is showing that microhardness of tracks first decreases

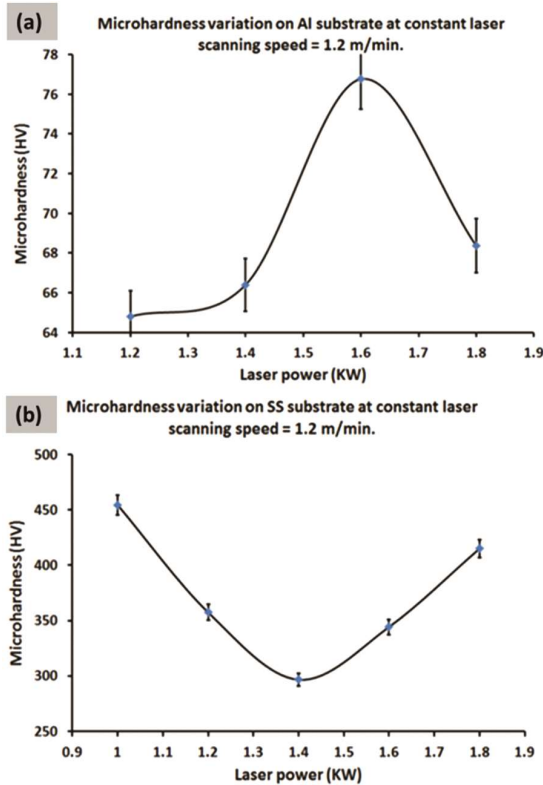


Fig. 11- Variation in microhardness with varying laser powers (a) Al substrate (sample no. 2), (b) SS substrate (sample no. 3).

up to 1.4 kW power and then increases. Fine microstructure results improved microhardness and dispersion of alloying element decide the microhardness<sup>23</sup>.

## Conclusion

This experiment concludes the optimized parameters of LAM for synthesis of Al + 1 wt. % graphene composite. The microstructural analysis of single deposited layers on different substrate (Al & SS316) with different combinations of process parameters is performed to identify the material deposition behaviour on the basis of track width and microhardness measurements. Microhardness of tracks varies simultaneously with various parameters such as porosity, graphene dispersion and cooling rate. Hence it is challenging to identify the effect of each single parameter on microhardness. A similar pattern of microhardness variation is observed i.e. first decreasing and then increasing that occurs may be due to the variation in peak temperature, cooling rate of melt pool and dispersion of graphene. Sometimes random behaviour in microhardness variation is observed that occurs may be due to the

inappropriate selection of process parameters and combined effect of porosity, graphene dispersion and cooling rate. It is observed that P/v ratio plays an important role in melting and deposition of material. For different deposited tracks the width increases as P/v ratio increases up to a limit and 400 J/mm is critical value of P/v above which material deposition reduces. Generally track width reduces with increase in scan speed and decrease in laser power but material deposition reduces when energy intensity is more than critical value.

Additive manufacturing of metal matrix composite is at infancy stage and present work enlightens the new path for synthesis of graphene metal matrix composites by laser additive manufacturing. LAM built Aluminium graphene composite have potential application in various industries. There are still some hidden facts which need to explore further for making graphene more useful in the area of light weight composites. Present work invites researcher to enhance the quality of graphene metal matrix composites and use graphene in metal matrix efficiently by additive manufacturing.

## Reference

- Bremen S, Meiners W & Diatlov A, *Laser Technik J*, 9 (2012) 33.
- Bartolo P, Jorge M A, Batista F C, Almeida H A, Matias J M, Vasco J C, Gaspar J B, Correia M A, Andre N C & Alves N F, *Virtual and rapid manufacturing: advanced research in virtual and rapid prototyping*, (CRC Press, 2007).
- Kruth J P, Froyen L, Vaerenbergh J V, Mercelis P, Rombouts M & Lauwers B, *J Mater Proc Technol*, 149 (2004) 616.
- Yadroitsev I, Bertrand P & Smurov I, *Appl Surf Sci*, 253 (2007) 8064.
- Simchi A, *Metall Mater Trans B*, 35 (2004) 937.
- Mumtaz K A, Erasenthiran P & Hopkinson N, *J Mater Process Technol*, 195 (2008) 77.
- Yadroitsev I & Smurov I, *Phys Proc*, 5 (2010) 551.
- Gu D & Shen Y, *J Alloys Compd*, 432 (2007) 163.
- Niu H J & Chang I T H, *Scripta Mater*, 41 (1999) 1229.
- Li R, Liu J, Shi Y, Wang L & Jiang W, *The Int J Adv Manuf Technol*, 59 (2012) 1025.
- Childs T H C, Hauser C & Badrossamay M, *CIRP Annals-Manufacturing Technology*, 53 (2004) 191.
- Dadbakhsh S, Hao L, Jerrard P G E & Zhang D Z, *Powder Technol*, 231 (2012) 112.
- Liu W & DuPont J N, *Scripta Mater*, 48 (2003) 1337.
- Shiva S, Palani I A, Paul C P, Mishra S K & Singh B, *J Mater Process Technol*, 238 (2016) 142.
- Thijs L, Verhaeghe F, Craeghs T, H J Van & Kruth J P, *Acta Materialia*, 58 (2010) 3303.
- Read N, Wang W, Essa K & Attallah M M, *Mater Des*, 65 (2015) 417.
- Qiu C, Yue S, Adkins N J E, Ward M, Hassanin H, Lee P D, Withers P J & Attallah M M, *Mater Sci Eng A*, 628 (2015) 188.

- 18 Aboulkhair N T, Everitt N M, Ashcroft I & Tuck C, *Addit Manuf*, 1 (2014) 77.
- 19 Wang X J, Zhang L C, Fang M H & Sercombe T B, *Mater Sci Eng A*, 597 (2014) 370.
- 20 Macleod H A, *Thin-film optical filters*, (CRC press, 2001).
- 21 ASM, 2014. ASM Material data sheet: Aluminum 6061-T6; 6061-T651, ASM Aerospace specification metals INC.
- 22 Paul C P, Ganesh P, Mishra S K, Bhargava P, Negi J & Nath A K, *Opt Laser Technol*, 39 (2007) 800.
- 23 Aboulkhair N T, Maskery I, Tuck C, Ashcroft I & Everitt N, In *Industrial Laser Applications Symposium 2015*, (International Society for Optics and Photonics: 2015) 965702-965702-7.